Volume 1
Number 4
October 2022
Pages 393–596

Environmental Science Advances

rsc.li/esadvances

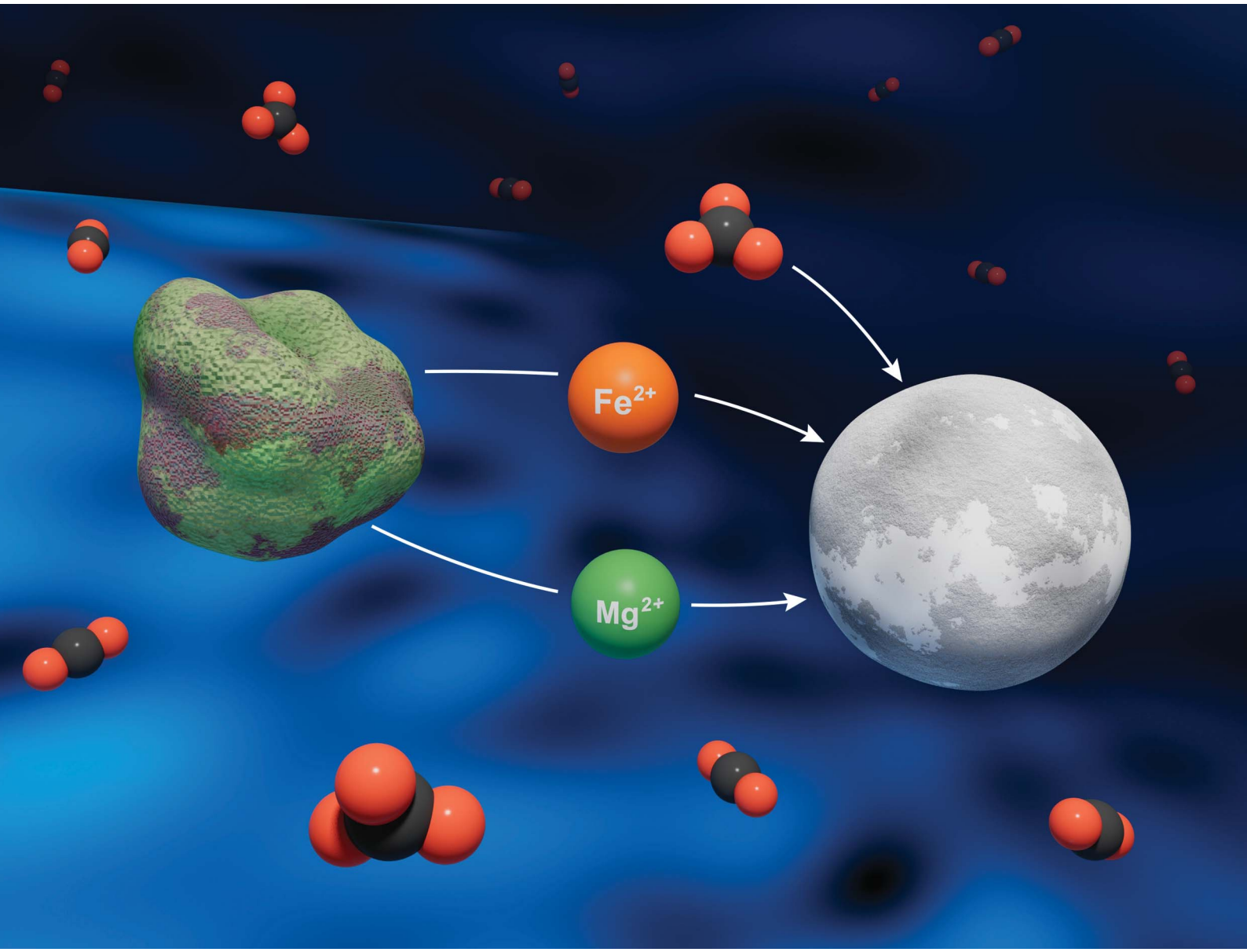

ISSN 2754-7000

ROYAL SOCIETY OF CHEMISTRY

COMMUNICATION

Quin R. S. Miller and H. Todd Schaef

Activation energy of magnesite ($MgCO_3$) precipitation: recent insights from olivine carbonation studies

Environmental Science Advances

ROYAL SOCIETY OF CHEMISTRY

COMMUNICATION

View Article Online
View Journal | View Issue

Check for updates

Cite this: *Environ. Sci.: Adv.*, 2022, **1**, 426

Received 8th April 2022
Accepted 8th July 2022

DOI: 10.1039/d2va00066k

rsc.li/esadvances

Activation energy of magnesite ($MgCO_3$) precipitation: recent insights from olivine carbonation studies

Quin R. S. Miller * and H. Todd Schaef *

We present two new activation energies for magnesite precipitation during forsteritic olivine ($Mg_{2-x}Fe_xSiO_4$; $0.18 \leq x \leq 0.26$) carbonation in high-pressure carbon dioxide. These new activation energies of 89 ± 6 and 85 ± 1 kJ mol^{-1} are consistent with the literature for magnesite precipitation in aqueous media and extend the temperature range to encompass 90 °C to 50 °C. These insights will help improve understanding of mineral transformation kinetics in the subsurface, including carbon storage in mafic-ultramafic environments, and aid in the development of carbon dioxide removal (CDR) and net negative-emissions technologies.

Environmental significance

Olivine is a key constituent of reactive geologic formations and industrial wastes that are targets for permanent carbon storage *via* mineralization. The relative paucity of kinetic parameters for olivine transformation to magnesite *via* coupled dissolution and carbonate precipitation hinders efforts to predict rate and design efficient mineralization strategies. Our calculations of two new olivine carbonation activation energies help address these knowledge gaps relevant to natural and engineered environmental carbon-management processes.

The concept of carbon dioxide removal (CDR) through carbon capture and sequestration is an integral component of current climate mitigation strategies and pursuit of net-negative emissions technologies. A promising CDR approach involves injection of carbon dioxide (CO_2) into reactive mafic and ultramafic rocks to form stable carbonate minerals, enabling rapid permanent carbon storage.[1–8] In this context, understanding rates of mineral carbonation is crucial for predicting fate and transport of subsurface CO_2.

Olivine ($Mg_{2-x}Fe_xSiO_4$) is a key reactive component of mafic and ultramafic rocks, and its dissolution, hydration, and carbonation rates have received considerable scrutiny (*c.f.*, ref. 9–13). The recent quantitative kinetics analyses and compilations of Miller *et al.*[11] and Sendula *et al.*[12] fit the Avrami model[14] and shrinking particle model (SPM),[12,15–17] respectively, to the broad olivine carbonation literature. The more recent and comprehensive study of Sendula *et al.*[12] provided 35 new experiments, nearly doubling the amount of available datasets, and the SPM proved most flexible and adaptable for the diverse olivine carbonation literature. The goal of the present Communication is to extract carbonation activation energy parameters from recently compiled olivine carbonation studies.[11,12] To do so we critically reviewed the datasets to identify two[12,18] suitable internally-consistent collections of reaction rate *vs.* temperature data for magnesite precipitation during olivine carbonation. These datasets were suitable as they included reaction kinetics for at least three distinct temperatures.

The San Carlos olivine used in Sendula *et al.*[12] has ~88–91% of the divalent metal sites occupied with Mg^{2+} (Fo_{88}–Fo_{91}; $Mg_{1.76}Fe_{0.24}SiO_4$ to $Mg_{1.82}Fe_{0.18}SiO_4$),[19–23] and the composition of the Gadikota *et al.*[18] olivine is Fo_{87}. The most rapid olivine carbonation occurs at ~185–200 °C. (*c.f.*, ref. 11 and 12) Indeed, the high-temperature datapoints of Sendula *et al.*[12] (200 °C) and Gadikota *et al.*[18] (185 °C) are lower than expected based on the calculated activation energies, consistent with this 185–200 °C temperature range being an inflection point for rate *vs.* temperature.

Plots of the Sendula *et al.*[12] (Se21, 50–150 °C) and Gadikota *et al.*[18] (Ga14, 90–150 °C) carbonation rates on Arrhenius plots (Fig. 1a and b) illustrate the linear relationships needed to calculate apparent activation energies. The linearity of the Arrhenius plots indicates that temperature is the dominant control, and other possible variations in chemical affinity and pressure[12] (Fig. 1c) are negligible, at least for these far-from-equilibrium high-pressure carbonation studies. The olivine to magnesite activation energy values are "apparent" as they encompass contributions from all elementary reactions involved in the complex dissolution–precipitation processes. The calculations revealed the apparent activation energies of 89 ± 6 (Se21) and 85 ± 1 (Ga14) kJ mol^{-1}. These newly-determined

Physical and Computational Sciences Directorate, Pacific Northwest National Laboratory, Richland, WA, USA. E-mail: quin.miller@pnnl.gov; todd.schaef@pnnl.gov

Open Access Article. Published on 18 Julie 2022. Downloaded on 2026-05-12 11:39:47 nm..
This article is licensed under a Creative Commons Attribution 3.0 Unported Licence.

© 2022 The Author(s). Published by the Royal Society of Chemistry

Open Access Article. Published on 18 Julie 2022. Downloaded on 2026-05-12 11:39:47 nm..
This article is licensed under a Creative Commons Attribution 3.0 Unported Licence.

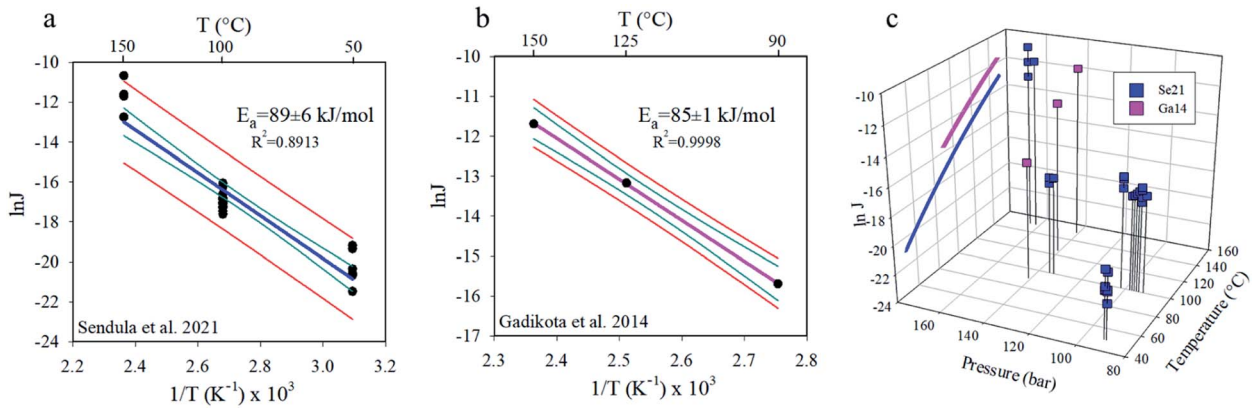

Fig. 1 Arrhenius plots using the carbonation rate results of (a) Sendula *et al.*[12] (Se21) and (b) Gadikota *et al.*[18] (Ga14), showing the variation of the natural logarithm of the olivine to magnesite transformation rates (J, mol m^{-2} s^{-1}) as a function of 1000 times the reciprocal absolute temperature (*T*) of the experiments. Temperature (°C) is labelled on the upper *x*-axis for reference. The calculated apparent activation energies, coefficient of determination, and uncertainties are given next to the linear best fits. Red and dark cyan curves denote 95% prediction band and 95% confidence bands, respectively. In panel (c), the Arrhenius trends have both been plotted on the °C *vs.* ln *J* plane, while the Sendula *et al.*[12] and Gadikota *et al.*[18] rates used to construct the Arrhenius plots are shown in the context of pressure and temperature conditions. The reference drop lines from the points to the P–T plane help clarify the 3D perspective.

activation energies are consistent with the literature for magnesite precipitation in aqueous media (Table 1). This present analysis extended the temperature range of the Table 1 dataset down from 90 °C to 50 °C. Although the studies compiled in Table 1 span a range of aqueous-mediated processes, including olivine carbonation, hydromagnesite transformation, and step advancement on magnesite, all values are presented given the paucity of literature data. Our group at Pacific Northwest National Laboratory has also studied the influence of adsorbed water nanofilm thickness on the activation energy of forsterite to magnesite carbonation, demonstrating a linear relationship between reported monolayer H_2O thickness and activation energy, from ~34 to ~130 kJ mol^{-1}.[24–26] Given the occurrence of multiphase CO_2–H_2O fluids, it is vital to understand the barriers to magnesite precipitation in aqueous media to predict and interpret experiments conducted in non-aqueous regimes (*e.g.*, water films).

In summary, this Communication presents two new robust activation energies for the olivine to magnesite carbonation reaction. These types of monomineralic studies are important for delineating controlling reaction mechanisms and kinetic interpretation of mafic-ultramafic rock carbonation studies (*e.g.* ref. 22, 27–35). Further insights from dynamic kinetic model[36] and reactive force-field[37,49] development, along with additional carbonation kinetics studies,[12,16,38–40] are vital for clarifying the multiscale mechanisms and rates of silicate carbonation

Table 1 Compiled apparent activation energies for magnesite precipitation in aqueous media

Magnesite ($MgCO_3$) precipitation apparent activation energies		
Activation energy (kJ mol^{-1})	Temperature (°C)	Ref.
Present communication		
89 ± 6	50–150	This study, based on olivine carbonation kinetics reported by Sendula *et al.*[12]
85 ± 1	90–150	This study, based on Sendula *et al.*[12] calculation of Gadikota *et al.*[18] olivine to magnesite carbonation rates
Literature values		
159 ± 17	90–100	Saldi *et al.* 2009 (ref. 41)
122.6 ± 20[a]	120–180	Di Lorenzo *et al.* 2014 (ref. 42)
100[a]	110–200	Zhang *et al.* 2000 (ref. 43)
93.3 ± 3.3[a]	120–180	Di Lorenzo *et al.* 2014 (ref. 42)
85.1 ± 7.7	100–146	Gautier *et al.* 2016 (ref. 44)
81[a]	110–200	Zhang *et al.* 2000 (ref. 43)
80.2	100–200	Saldi *et al.* 2012 (ref. 45)
92.9 ± 3.8[b]	15–35[b]	Arvidson and Mackenzie 2000 (ref. 46)

[a] Based on the solution-mediated transformation reaction of hydromagnesite [$(Mg_5(CO_3)_4(OH)_2 \cdot 4H_2O)$] to magnesite. Multiple Zhang *et al.*[43] values are due to different fluid compositions, and multiple values for Di Lorenzo *et al.*[42] were due to their use of two different kinetic models. [b] Arvidson and Mackenzie[46] used the approach of Lippmann[47] in conjunction with the 39.3 kJ mol^{-1} calcite ($CaCO_3$) activation energy of Kazmierczak *et al.*[48] to calculate their magnesite precipitation activation energy.

© 2022 The Author(s). Published by the Royal Society of Chemistry

Open Access Article. Published on 18 Julie 2022. Downloaded on 2026-05-12 11:39:47 nm..
This article is licensed under a Creative Commons Attribution 3.0 Unported Licence.

transformations. Our analysis provides a basis for focusing future work on key mechanistic and kinetic unknowns that could improve understanding of mineral transformation kinetics in the subsurface, including carbon storage in mafic–ultramafic rocks, and aid in the development of carbon dioxide removal and net negative-emissions technologies.

Conflicts of interest

There are no conflicts of interest.

Acknowledgements

QRSM was supported by the U.S. Department of Energy (DOE), Office of Science, Office of Basic Energy Sciences (BES), Chemical Sciences, Geosciences, and Biosciences Division through its Geosciences program at Pacific Northwest National Laboratory (PNNL). HTS was supported by the U.S. Department of Energy's Carbon Storage Program and thanks Darin Damiani from DOE-HQ. HTS also acknowledges partial support from the Carbon Utilization and Storage Partnership (CUSP). We also thank the three anonymous reviewers for their close attention and helpful comments.

References

1 B. P. McGrail, F. A. Spane, E. C. Sullivan, D. H. Bacon and G. Hund, The Wallula Basalt Sequestration Pilot Project, *Energy Procedia*, 2011, **4**, 5653–5660.
2 B. P. McGrail, H. T. Schaef, A. M. Ho, Y.-J. Chien, J. J. Dooley and C. L. Davidson, Potential for carbon dioxide sequestration in flood basalts, *J. Geophys. Res.: Solid Earth*, 2006, **111**, B12.
3 H. T. Schaef, B. P. McGrail and A. T. Owen, Carbonate mineralization of volcanic province basalts, *Int. J. Greenhouse Gas Control*, 2010, **4**, 249–261.
4 J. M. Matter and P. B. Kelemen, Permanent storage of carbon dioxide in geological reservoirs by mineral carbonation, *Nat. Geosci.*, 2009, **2**, 837–841.
5 B. P. McGrail, H. T. Schaef, F. A. Spane, J. B. Cliff, O. Qafoku, J. A. Horner, C. J. Thompson, A. T. Owen and C. E. Sullivan, Field validation of supercritical CO_2 reactivity with basalts, *Environ. Sci. Technol. Lett.*, 2017, **4**, 6–10.
6 J. M. Matter, M. Stute, S. Ó. Snæbjörnsdottir, E. H. Oelkers, S. R. Gislason, E. S. Aradottir, B. Sigfusson, I. Gunnarsson, H. Sigurdardottir, E. Gunnlaugsson, G. Axelsson, H. A. Alfredsson, D. Wolff-Boenisch, K. Mesfin, D. F. d. l. R. Taya, J. Hall, K. Dideriksen and W. S. Broecker, Rapid carbon mineralization for permanent disposal of anthropogenic carbon dioxide emissions, *Science*, 2016, **352**, 1312–1314.
7 B. M. Tutolo, A. Awolayo and C. Brown, Alkalinity Generation Constraints on Basalt Carbonation for Carbon Dioxide Removal at the Gigaton-per-Year Scale, *Environ. Sci. Technol.*, 2021, **55**, 11906–11915.
8 S. K. White, F. A. Spane, H. T. Schaef, Q. R. S. Miller, M. D. White, J. A. Horner and B. P. McGrail, Quantification of CO_2 Mineralization at the Wallula Basalt Pilot Project, *Environ. Sci. Technol.*, 2020, **54**, 14609–14616.
9 E. H. Oelkers, J. Declercq, G. D. Saldi, S. R. Gislason and J. Schott, Olivine dissolution rates: A critical review, *Chem. Geol.*, 2018, **500**, 1–19.
10 J. D. Rimstidt, S. L. Brantley and A. A. Olsen, Systematic review of forsterite dissolution rate data, *Geochim. Cosmochim. Acta*, 2012, **99**, 159–178.
11 Q. R. S. Miller, H. T. Schaef, J. P. Kaszuba, G. Gadikota, B. P. McGrail and K. M. Rosso, Quantitative Review of Olivine Carbonation Kinetics: Reactivity Trends, Mechanistic Insights, and Research Frontiers, *Environ. Sci. Technol. Lett.*, 2019, **6**, 431–442.
12 E. Sendula, H. M. Lamadrid, J. D. Rimstidt, M. Steele-MacInnis, D. M. Sublett, L. E. Aradi, C. Szabó, M. J. Caddick, Z. Zajacz and R. J. Bodnar, Synthetic Fluid Inclusions XXIV. *In situ* Monitoring of the Carbonation of Olivine Under Conditions Relevant to Carbon Capture and Storage Using Synthetic Fluid Inclusion Micro-Reactors: Determination of Reaction Rates, *Front. Clim.*, 2021, **3**, 722447.
13 H. M. Lamadrid, Z. Zajacz, F. Klein and R. J. Bodnar, Synthetic fluid inclusions XXIII. Effect of temperature and fluid composition on rates of serpentinization of olivine, *Geochim. Cosmochim. Acta*, 2021, **292**, 285–308.
14 M. Avrami, Kinetics of Phase Change. II Transformation-Time Relations for Random Distribution of Nuclei, *J. Chem. Phys.*, 1940, **8**, 212–224.
15 H. M. Lamadrid, J. D. Rimstidt, E. M. Schwarzenbach, F. Klein, S. Ulrich, A. Dolocan and R. J. Bodnar, Effect of water activity on rates of serpentinization of olivine, *Nat. Commun.*, 2017, **8**, 16107.
16 E. Sendula, H. M. Lamadrid and R. J. Bodnar, Reaction Rates Of Olivine Carbonation-An Experimental Study Using Synthetic Fluid Inclusions As Micro-Reactors, *AGU Fall Meeting Abstracts*, 2017, 2017AGUFMOS2053D1243S, **https://ui.adsabs.harvard.edu/abs/2017AGUFMOS2053D1243S/abstract**.
17 J. D. Rimstidt, *Geochemical Rate Models: An Introduction to Geochemical Kinetics*, Cambridge University Press, 2013.
18 G. Gadikota, J. Matter, P. Kelemen and A.-h. A. Park, Chemical and morphological changes during olivine carbonation for CO_2 storage in the presence of NaCl and $NaHCO_3$, *Phys. Chem. Chem. Phys.*, 2014, **16**, 4679–4693.
19 H. Ueda, Y. Sawaki and S. Maruyama, Reactions between olivine and CO_2-rich seawater at 300 °C: Implications for H_2 generation and CO_2 sequestration on the early Earth, *Geosci. Front.*, 2017, **8**, 387–396.
20 F. Klein and T. M. McCollom, From serpentinization to carbonation: New insights from a CO_2 injection experiment, *Earth Planet. Sci. Lett.*, 2013, **379**, 137–145.
21 Y. Sekine, T. Shibuya, F. Postberg, H. W. Hsu, K. Suzuki, Y. Masaki, T. Kuwatani, M. Mori, P. K. Hong, M. Yoshizaki, S. Tachibana and S. Sirono, High-temperature water-rock interactions and hydrothermal environments in the chondrite-like core of Enceladus, *Nat. Commun.*, 2015, **6**, 8604.

© 2022 The Author(s). Published by the Royal Society of Chemistry

Open Access Article. Published on 18 Julie 2022. Downloaded on 2026-05-12 11:39:47 nm..
This article is licensed under a Creative Commons Attribution 3.0 Unported Licence.

22 O. Sissmann, F. Brunet, I. Martinez, F. Guyot, A. Verlaguet, Y. Pinquier and D. Daval, Enhanced Olivine Carbonation within a Basalt as Compared to Single-Phase Experiments: Reevaluating the Potential of CO_2 Mineral Sequestration, *Environ. Sci. Technol.*, 2014, **48**, 5512–5519.

23 R. Lafay, G. Montes-Hernandez, E. Janots, R. Chiriac, N. Findling and F. Toche, Simultaneous precipitation of magnesite and lizardite from hydrothermal alteration of olivine under high-carbonate alkalinity, *Chem. Geol.*, 2014, **368**, 63–75.

24 Q. R. S. Miller, J. P. Kaszuba, H. T. Schaef, M. E. Bowden, B. P. McGrail and K. M. Rosso, Anomalously low activation energy of nanoconfined $MgCO_3$ precipitation, *Chem. Commun.*, 2019, **55**, 6835–6837.

25 Q. R. S. Miller, J. P. Kaszuba, S. N. Kerisit, H. T. Schaef, M. E. Bowden, B. P. McGrail and K. M. Rosso, Emerging investigator series: ion diffusivities in nanoconfined interfacial water films contribute to mineral carbonation thresholds, *Environ. Sci.: Nano*, 2020, **7**, 1068–1081.

26 S. N. Kerisit, S. T. Mergelsberg, C. J. Thompson, S. K. White and J. S. Loring, Thin Water Films Enable Low-Temperature Magnesite Growth Under Conditions Relevant to Geologic Carbon Sequestration, *Environ. Sci. Technol.*, 2021, **55**, 12539–12548.

27 J. Hovelmann, H. Austrheim and B. Jamtveit, Microstructure and porosity evolution during experimental carbonation of a natural peridotite, *Chem. Geol.*, 2012, **334**, 254–265.

28 A. P. Gysi and A. Stefánsson, CO_2-water–basalt interaction. Low temperature experiments and implications for CO_2 sequestration into basalts, *Geochim. Cosmochim. Acta*, 2012, **81**, 129–152.

29 R. J. Rosenbauer, B. Thomas, J. L. Bischoff and J. Palandri, Carbon sequestration *via* reaction with basaltic rocks: Geochemical modeling and experimental results, *Geochim. Cosmochim. Acta*, 2012, **89**, 116–133.

30 H. Ueda, T. Shibuya, Y. Sawaki, M. Saitoh, K. Takai and S. Maruyama, Reactions between komatiite and CO_2-rich seawater at 250 and 350 °C, 500 bars: implications for hydrogen generation in the Hadean seafloor hydrothermal system, *Prog. Earth Planet. Sci.*, 2016, **3**, 35.

31 T. Shibuya, M. Yoshizaki, Y. Masaki, K. Suzuki, K. Takai and M. J. Russell, Reactions between basalt and CO_2-rich seawater at 250 and 350 °C, 500 bars: Implications for the CO_2 sequestration into the modern oceanic crust and the composition of hydrothermal vent fluid in the CO_2-rich early ocean, *Chem. Geol.*, 2013, **359**, 1–9.

32 N. G. Grozeva, F. Klein, J. S. Seewald and S. P. Sylva, Experimental study of carbonate formation in oceanic peridotite, *Geochim. Cosmochim. Acta*, 2017, **199**, 264–286.

33 A. J. Luhmann, B. M. Tutolo, B. C. Bagley, D. F. Mildner, P. P. Scheuermann, J. M. Feinberg, K. Ignatyev and W. E. Seyfried Jr, Chemical and physical changes during seawater flow through intact dunite cores: An experimental study at 150–200 °C, *Geochim. Cosmochim. Acta*, 2017, **214**, 86–114.

34 A. J. Luhmann, B. M. Tutolo, B. C. Bagley, D. F. Mildner, W. E. Seyfried and M. O. Saar, Permeability, porosity, and mineral surface area changes in basalt cores induced by reactive transport of CO_2-rich brine, *Water Resour. Res.*, 2017, **53**, 1908–1927.

35 A. J. Luhmann, B. M. Tutolo, C. Y. Tan, B. M. Moskowitz, M. O. Saar and W. E. Seyfried, Whole rock basalt alteration from CO_2-rich brine during flow-through experiments at 150 °C and 150 bar, *Chem. Geol.*, 2017, **453**, 92–110.

36 A. M. Bremen, T. Ploch, A. Mhamdi and A. Mitsos, A mechanistic model of direct forsterite carbonation, *Chem. Eng. J.*, 2021, **404**, 126480.

37 S. Zare and M. J. A. Qomi, Reactive force fields for aqueous and interfacial magnesium carbonate formation, *Phys. Chem. Chem. Phys.*, 2021, **23**, 23106–23123.

38 F. Wang, D. Dreisinger, M. Jarvis and T. Hitchins, Kinetics and mechanism of mineral carbonation of olivine for CO_2 sequestration, *Miner. Eng.*, 2019, **131**, 185–197.

39 F. Wang, D. Dreisinger, M. Jarvis and T. Hitchins, Kinetic evaluation of mineral carbonation of natural silicate samples, *Chem. Eng. J.*, 2021, **404**, 126522.

40 F. Wang, D. Dreisinger, M. Jarvis, T. Hitchins and D. Dyson, Quantifying kinetics of mineralization of carbon dioxide by olivine under moderate conditions, *Chem. Eng. J.*, 2019, **360**, 452–463.

41 G. D. Saldi, G. Jordan, J. Schott and E. H. Oelkers, Magnesite growth rates as a function of temperature and saturation state, *Geochim. Cosmochim. Acta*, 2009, **73**, 5646–5657.

42 F. Di Lorenzo, R. M. Rodriguez-Galan and M. Prieto, Kinetics of the solvent-mediated transformation of hydromagnesite into magnesite at different temperatures, *Mines Mag.*, 2014, **78**, 1363–1372.

43 P. Zhang, H. L. Anderson, J. W. Kelly, J. L. Krumhansl and H. W. Papenguth, Kinetics and mechanisms of formation of magnesite from hydromagnesite in brine, *Technical Report SAN099-19465*, Sandia National Labs., Albuquerque, NM (US), 2000.

44 Q. Gautier, P. Benezeth and J. Schott, Magnesite growth inhibition by organic ligands: An experimental study at 100, 120 and 146 °C, *Geochim. Cosmochim. Acta*, 2016, **181**, 101–125.

45 G. D. Saldi, J. Schott, O. S. Pokrovsky, Q. Gautier and E. H. Oelkers, An experimental study of magnesite precipitation rates at neutral to alkaline conditions and 100-200 °C as a function of pH, aqueous solution composition and chemical affinity, *Geochim. Cosmochim. Acta*, 2012, **83**, 93–109.

46 R. S. Arvidson and F. T. Mackenzie, Temperature dependence of mineral precipitation rates along the $CaCO_3$-$MgCO_3$ join, *Aquat. Geochem.*, 2000, **6**, 249–256.

47 F. Lippmann, *Sedimentary Carbonate Minerals*, Springer Berlin Heidelberg, Berlin, Heidelberg, 1973.

48 T. F. Kazmierczak, M. B. Tomson and G. H. Nancollas, Crystal growth of calcium carbonate. A controlled composition kinetic study, *J. Phys. Chem.*, 1982, **86**, 103–107.

49 S. Zare, Formation and Dissolution of Surface Metal Carbonate Complexes: Implications for Interfacial Carbon Mineralization in Metal Silicates, *J. Phys. Chem. C*, 2022, DOI: **10.1021/acs.jpcc.2c02981**.